

# Egocentric physics : just about Mie

Brian Stout<sup>1</sup> and Ross McPhedran<sup>2</sup>

<sup>1</sup>*Aix-Marseille Université, CNRS, Centrale Marseille, Institut Fresnel,  
Campus de Saint Jérôme, 13397 Marseille, France \* and*

<sup>2</sup>*CUDOS, School of Physics, University of Sydney, 2006, Australia.*

We show that the physics of anapole excitations can be accurately described in terms of a resonant state expansion formulation of standard Mie theory without recourse to Cartesian coordinate based ‘toroidal’ currents that have previously been used to describe this phenomenon. In this purely Mie theory framework, the anapole behavior arises as a result of a Fano-type interference effect between different quasi-normal modes of the scatterer that effectively eliminate the scattered field in the associated multipole order.

## I. INTRODUCTION

Modern research in metamaterials and nanotechnology often seeks to exploit the considerable variety in the behaviors of open nano resonator systems. Despite the complexity of such systems, there has been a growing appreciation of the fact that their behavior near a resonance can be described in terms of a small number of parameters within frameworks satisfying general physical principles like energy conservation, reciprocity, and time reversal<sup>1,2</sup>. There is also an increasing interest in exploiting the resonances of high-index dielectrics for metamaterial and sensing applications in order to circumvent the problems caused by losses in metallic resonators at optical and near-optical frequencies<sup>3-5</sup>.

An interesting topic arising in the applications and theory of high-index optical nanosystems is that of anapole resonances, in which the fields generated by polarization currents inside high index dielectric spheres interfere in such a manner that their superposition radiates little energy outside the sphere<sup>3-5</sup>. Recently, doubt has been raised as to whether or not the conventional basis of the classic modes of Mie scattering theory is well adapted to describe these anapole resonances<sup>6</sup>, or whether it is better to describe fields in terms of a combination of Mie modes and the alternative toroidal modes<sup>1,3,4</sup>. Here we will show that the slow convergence of the Mie basis reported by Powell<sup>6</sup> can be readily remedied by incorporating an extra, analytically-determined phase factor, arising in the theory of product representations of functions of a complex variable<sup>7</sup>. With this extra factor included, we show that just two resonant modes from Mie theory are sufficient to give an accurate representation of the anapole resonance in a case from the literature<sup>3</sup>.

The  $\exp(-i\omega t)$  convention for time harmonic fields will be used for throughout this work. It is also convenient to express formulas in terms of the particle size parameter,  $z$ , with respect to the external ‘background’ media, *i.e.*  $z \equiv kR$  with  $k \equiv \frac{\omega}{c} \sqrt{\varepsilon_{r,b} \mu_{r,b}} \equiv N_b \frac{\omega}{c}$ , the wavenumber in the background media.

## II. ANAPOLE ‘MODES’

Anapole ‘modes’ of a scatterer have generally been described in the context of high index dielectrics. As our first example, we consider a pure dielectric sphere model with a permittivity index near that of silicon,  $\varepsilon_s = 16$ , for an incident wavelength of  $\lambda = 550\text{nm}$  that has already been shown to possess an anapole behavior<sup>3</sup>. The total cross section,  $\sigma$ , divided by the geometric cross section,  $\pi R^2$ , plotted in Fig.1, is the sum of all the individual multipole contributions of both electric or magnetic wave types. The ‘anapole’ condition for the electric dipole mode occurs when its contribution to the total cross section is zero, which as can be seen from the figure occurs at  $D \sim 204\text{nm}$ .

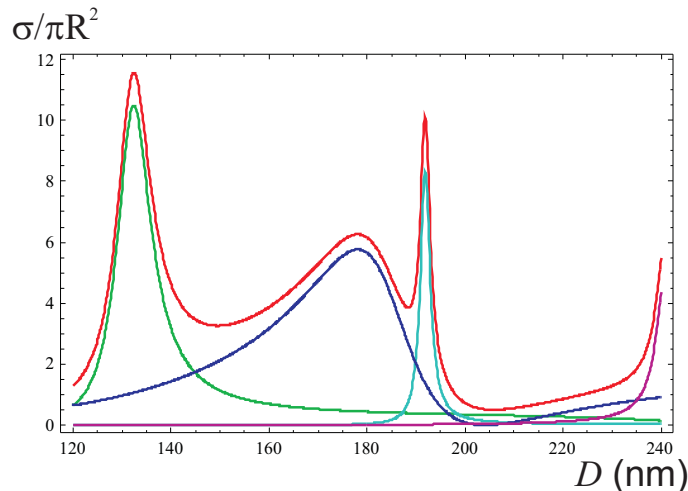


FIG. 1: Cross section versus particle diameter in nano-meters for a sphere of permittivity,  $\varepsilon_s=16$  with a background wavelength of  $\lambda = 550\text{nm}$ . Total cross section is plotted in red. The electric dipole cross section exhibiting anapole behavior is plotted in blue, with magnetic dipole contribution in green and magnetic quadrupole in cyan.

Each individual contribution to the cross section in Fig.1 was calculated from its corresponding  $S$ -function,  $S_n$ , via the formula,

$$\frac{\sigma_n}{\pi R^2} = \frac{2n+1}{z^2} \Re \{1 - S_n\} , \quad (1)$$

where the  $S_n$  have exact Mie theory expressions (given in eq.(18) of the appendixVI).

The  $S_n$  functions can alternatively be expressed in terms of a Weierstrass type product expansion in terms of the resonant state frequencies,  $\omega_\alpha$ , or equivalently resonant state size parameters,  $z_\alpha \equiv k_\alpha R \equiv N_b \omega_\alpha R/c$ . For each multipolar order and wave type, the  $z_\alpha$  can be readily determined as zeros of the transcendental equations in eq.(20), with the  $S_n$  function taking the form,

$$S_n(z) = (-)^{n+1} e^{-2iz} \prod_{\alpha=-\infty}^{\infty} \frac{z - z_{n,\alpha}^*}{z - z_{n,\alpha}} \quad (2)$$

$$= (-)^{n+1} e^{-2iz} \prod_{\alpha=1}^{\infty} \frac{z^2 - |z_{n,\alpha}|^2 + 2iz\text{Im}(z_{n,\alpha})}{z^2 - |z_{n,\alpha}|^2 - 2iz\text{Im}(z_{n,\alpha})},$$

where the  $e^{-2iz}$  phase factor is associated with causality. (This phase factor can be expressed either in terms of a sum over the difference between the  $z$  values of zeros and poles, summed over the entire set, or obtained in a more general way using causality - see King<sup>8</sup> Vol.2.) In the first line of eq.(2), time-reversal symmetry requires a symmetry between negative and positive resonant state eigenvalues,

$$-z_{n,-\alpha}^* = z_{n,\alpha}, \quad (3)$$

while in the last line of eq.(2) this symmetry is exploited to remove explicit reference to the negative energy resonant states. We remark that eq.(2) is only valid as it stands for dielectric scatterers (the zeros of  $S_n$  are not the complex conjugates of the resonant state values for dispersive media), and that eq.(2) is the form applicable to electric (TM) modes (*magnetic (TE)* product expressions are in fact identical *but of opposite sign* with a  $(-)^n$  prefactor).

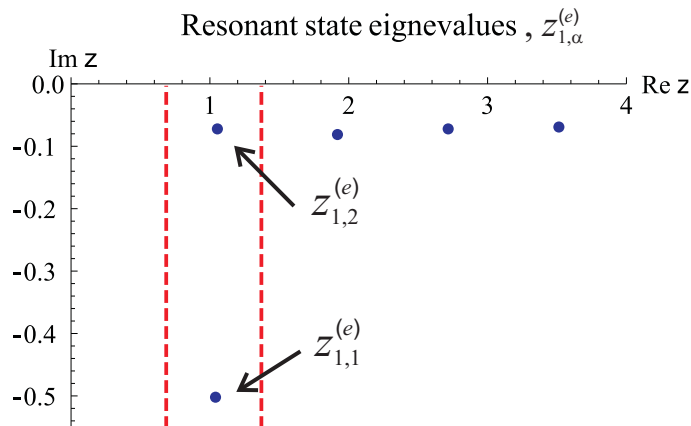


FIG. 2: Size parameter eigenvalues of the electric dipole resonant states,  $z_{1,\alpha}^{(e)}$ , for a sphere of permittivity,  $\epsilon_s=16$ . Vertical dashed lines delimit the size parameter range evaluated in Fig.1

From here on we concentrate attention on the electric dipole response since it exhibits anapole behavior. The electric dipole resonant states with the six lowest real parts are plotted in Fig.2 where the  $z_{n,\alpha}$  are obtained by solving for the zeros of the transcendental expression in eq.(20a). We immediately see from Fig.2 that there are two electric dipole resonant states in the diameter range explored in Fig.1 (region between the dashed vertical lines). Their values are  $z_1 \simeq 1.039 - i0.501$ , with a rather large imaginary part and  $z_2 \simeq 1.053 - i0.0723$  close to the real  $z$  axis.

The total electric dipole cross section (blue curve) is plotted in Fig.3, over the same  $D = 120$  to  $240$ nm range at  $\lambda_0 = 550$ nm, as in Fig.1 but with size parameter indicated on the ordinate in order to facilitate the comparison with Fig.2. The blue curve is the total electric dipole cross section. The red curve in Fig.3 is obtained if we only include the  $z_1$  contribution to the product expansion of  $S_1^{(e)}(z)$ , while the green curve is obtained by including both  $z_1$  and  $z_2$  in the  $S$ -function product expansion of eq.(2). The addition of the higher resonant states makes  $\sigma_1^{(e)}(z)$  rather slowly converge to the exact blue curve.

We now compare the expression (2) restricted to just the two dipole terms of the previous paragraph,

$$\sigma_1(z) \propto 2\Re \left[ 1 - \exp(-2iz) \frac{(z - z_{1,1}^*)(z - z_{1,2}^*)}{(z - z_{1,1})(z - z_{1,2})} \right], \quad (4)$$

with the calculations of Miroschnichenko A.E. *et al*<sup>3</sup> incorporating both Cartesian electric and toroidal dipoles- see Fig. 4. The simple expression (4) with the exponential factor present does very well in predicting the whole of the

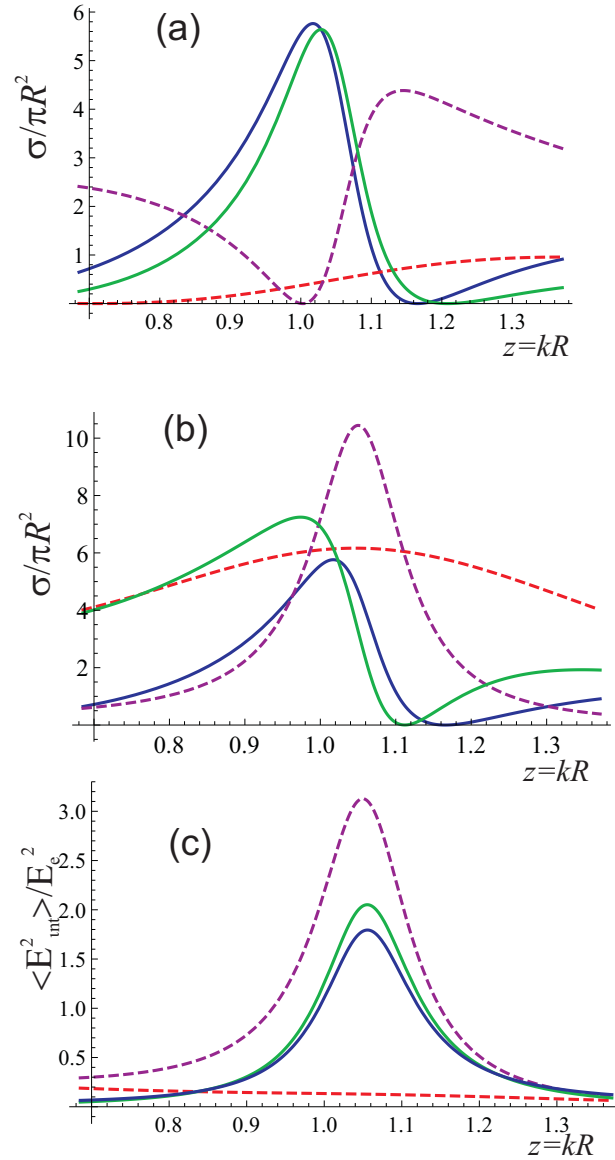


FIG. 3: Electric dipole cross section, (a)-(b), and average internal field enhancement, (c). Total contributions as blue curves. Dashed red curve in (a) and (c) corresponds to including only the  $z_{1,1}^{(e)}$  resonant state, while in (b) it corresponds to a superposition of the non-resonant contribution and the  $z_{1,1}^{(e)}$  resonant state. The dashed purple lines in (a)-(c) correspond to inclusion of only the  $z_{1,2}^{(e)}$  contributions. The green curves correspond to a coherent sum of  $z_{1,1}^{(e)}$  and  $z_{1,2}^{(e)}$  resonant states.

curve after the resonant maximum, through the anapole minimum and right to the large diameter end of the figure. Without the exponential factor, the two-term theory is totally inadequate. With the exponential factor, there is no need to incorporate toroidal terms in the Mie theory, in predicting the anapole minimum.

Although Figs.3(a) and 4 establish that both the  $z_1$  and  $z_2$  resonant states are required to reproduce the anapole behavior, product expansions don't readily lend themselves to the more familiar explanations of the Fano shape as an interference effect. This more traditional reasoning is obtainable by reformulating the cross section contributions as a resonant state sums of the Mie 'coefficients',  $a_n$  and  $b_n$ , (which are opposite in sign from the  $T_n$ -functions), given in eq.(18) of the appendix. The  $T_n$ -functions by definition relate the coefficients of the incident field to those of the

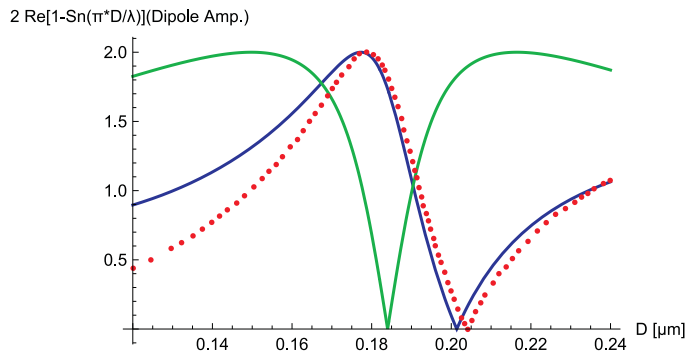


FIG. 4: The product form expression based on the two dipole mode expression (4) (blue curve) and the same without the exponential factor (green curve), compared with digitized points from Fig.2 of Miroschnichenko *et al*<sup>3</sup> (red points). Diameter varies from 120 to 240 nm at  $\lambda_0 = 550$ nm.

scattered field as in eq.(14), and are consequently related to the  $S_n$  functions via  $S_n = 1 + 2T_n$ , and contribute to the scattering cross section via the relation,

$$\frac{\sigma_n}{\pi R^2} = \frac{2n+1}{z^2} 2 |T_n|^2 . \quad (5)$$

The  $T_n$  functions can be expressed as a the sum of a non-resonant term plus a sum over the resonant state responses,

$$\begin{aligned} T_n(z) &= \frac{(-)^{n+1} e^{-2iz} - 1}{2} + \frac{(-)^{n+1} e^{-2iz}}{2} \sum_{\alpha=-\infty}^{\infty} \frac{r_{n,\alpha}}{z - z_{n,\alpha}} \\ &= \frac{(-)^{n+1} e^{-2iz} - 1}{2} \\ &\quad + (-)^{n+1} e^{-2iz} \sum_{\alpha=1}^{\infty} \frac{iz \text{Im}(r_{n,\alpha}) + \text{Re}(r_{n,\alpha} z_{n,\alpha}^*)}{z^2 - |z_{n,\alpha}|^2 - 2iz \text{Im}(z_{n,\alpha})} , \end{aligned} \quad (6)$$

where in the last line we used the fact that time reversal symmetry imposes the following relation on the residue factors,

$$r_{n,-\alpha} = -r_{n,\alpha}^* , \quad (7)$$

in order to eliminate summing over the negative energy states.

We remark that unlike the product form of eq.(2), the sum formulation of eq.(6) requires a calculation of the residues,  $r_{n,\alpha}$ . The  $r_{n,\alpha}$  can be obtained in a number of different manners: directly from eq.(2) if one has determined a sufficiently high number of resonant states, analytically via Mie theory and the Cauchy principal value theorem as given in eq.(25), or from far field information. For the same,  $\epsilon_s = 16$ , permittivity as in Figs.2 and 3, the residues associated with the first two resonant states are  $r_1 = -0.474 - 1.740i$  and  $r_2 = 0.0376 + 0.1996i$  so that even though the  $z_1$  mode is far from the real axis, it cannot be neglected on account of its large residue strength. We plot the total electric dipole cross section in Fig.3. The red curve is obtained by taking the sum in eq.(6) of the non-resonant contribution plus the broad  $z_1$  resonant state contribution. Adding in the the  $z_2$  resonant state contribution results in the green curve while the purple curve was obtained by treating the  $z_2$  contribution in isolation. We thus see that the anapole behavior has been predominantly recovered as a Fano type interference phenomenon between narrow and broad modes. To fully understand anapoles, we need to see how the field inside the particle is modified with respect to that which would exist in its absence, as discussed below.

### III. INTERNAL FIELD AVERAGES

The functions determining the linear relationship between internal and excitation field coefficients, are denoted  $\Omega_n$ , cf. eq.(16) (these are commonly called the  $c_n$  and  $d_n$  coefficients in Mie theory for TM and TE modes respectively). They can be written as a sum of resonant state Lorentzians like the  $T$ -matrix expression in eq.(6), (without the

non-resonant contributions),

$$\begin{aligned}\Omega_n &= \frac{(-)^{n+1} e^{-2iz}}{2} \sum_{\alpha=-\infty}^{\infty} \frac{r_{n,\alpha}^{(\Omega)}}{z - z_{n,\alpha}} \\ &= (-)^{n+1} e^{-2iz} \sum_{\alpha=1}^{\infty} \frac{iz \operatorname{Im} \left( r_{n,\alpha}^{(\Omega)} \right) + \operatorname{Re} \left( r_{n,\alpha}^{(\Omega)} z_{n,\alpha}^* \right)}{z^2 - |z_{n,\alpha}|^2 - 2iz \operatorname{Im} (z_{n,\alpha})}.\end{aligned}\quad (8)$$

The residue factors,  $r_{n,\alpha}^{(\Omega)}$ , differ from those of the  $T$ -matrix, and can be calculated analytically in Mie theory, and are given in eq.(24).

Although we know of no precise analogue of cross section for the internal field, the volume average of the internal field intensity divided by excitation field intensity at the spheres center is a physically relevant quantity which also has additive multipole contributions,

$$\begin{aligned}\frac{\langle \|\mathbf{E}^{(\text{int})}\|^2 \rangle_{V_s}}{\|\mathbf{E}_e(\mathbf{0})\|^2} &= \\ &= \frac{3}{2z^3} \sum_{n=1}^{\infty} (2n+1) \left\{ I_n |\Omega_n^{(e)}|^2 + J_n |\Omega_n^{(h)}|^2 \right\},\end{aligned}\quad (9)$$

where  $I_n$  and  $J_n$  arise from analytical integrations of the field squared, (see eq.(27b) of the appendix). We see in Fig.(3c) that the isolated contribution of the  $z_{1,1}^{(e)}$  resonant state to the internal field intensity is considerably smaller than that of the  $z_{1,2}^{(e)}$  state, but their superposition is still required to reasonably approximate the total average field intensity. We remark from Fig.(3c) that the internal field resonance is still significant at the anapole size parameter of  $z_{\text{anap}} \simeq 1.16$ .

#### IV. RESONANT STATE FIELD EXPANSIONS

As we have seen above, physically relevant quantities like cross sections and field averages can be formulated entirely in terms of the resonant frequencies and residues without explicit reference to the resonant state fields themselves. Nevertheless, in applications, like LDOS, Lamb shift, and the present analysis of ‘‘toroidal’’ currents, it is desirable to develop the field distribution directly in terms of the resonant states.

Mie theory provides an analytic expression for the multipolar component of the electric field inside the sphere originating from electric modes,  $\mathbf{E}_{n,m}^{(\text{int},e)}$ , which can be determined from eqs.(15a) and (16),

$$\mathbf{E}_{n,m}^{(\text{int},e)} = E e_{n,m} \Omega_n^{(e)} k^{3/2} \mathbf{N}_{n,m}^{(1)}(k_s \mathbf{r}), \quad (10)$$

where  $e_{n,m}$  is the multipolar excitation field coefficient determined for a field of amplitude of  $k^{3/2}$  at the origin, and  $E$  is a field amplitude parameter<sup>11</sup>. The resonant state expansion of  $\mathbf{E}_{n,m}^{(\text{int})}$  is,

$$\mathbf{E}_{n,m}^{(\text{int},e)} = \frac{(-)^{n+1} e^{-2iz} E e_{n,m}}{2} \sum_{\alpha=-\infty}^{\infty} \frac{r_{n,\alpha}^{(\Omega)}}{z - z_{n,\alpha}} \mathbf{E}_{n,m,\alpha}^{(\text{int},e)}, \quad (11)$$

where  $\mathbf{E}_{n,m,\alpha}^{(\text{int},e)}$  are the resonant state wave functions of the electric  $n, m$  multipolar mode, for which the analytical expressions in the case of a homogeneous sphere are,

$$\begin{aligned}\mathbf{E}_{n,m,\alpha}^{(\text{int},e)}(\mathbf{r}) &= \left[ \sqrt{n(n+1)} j_n(\rho_s z_{n,\alpha} \tilde{r}) \mathbf{Y}_{n,m}(\theta, \phi) \right. \\ &\quad \left. + \psi_n'(\rho_s z_{n,\alpha} \tilde{r}) \mathbf{Z}_{n,m}(\theta, \phi) \right] \frac{k_{n,\alpha}^{3/2}}{\rho_s z_{n,\alpha} \tilde{r}},\end{aligned}\quad (12)$$

where  $\mathbf{Y}_{n,m}$  and  $\mathbf{Z}_{n,m}$  are normalized vector spherical harmonics<sup>12</sup>. In eq.(12),  $\rho_s$  is the refractive index contrast of the sphere (cf. eq.(22)), and  $\tilde{r} \equiv r/R$  is a dimensionless radial coordinate normalized with respect to the sphere’s radius ( $\tilde{r} \leq 1$ ).

The real part of the electric field lines from Mie theory are plotted in Fig.5 on a background of an electric field intensity plot at the anapole point. One sees that there is indeed a ‘‘toroidal’’ aspect to the induced polarization currents, but these are completely described within the context of Mie theory without the need for any additional basis functions.

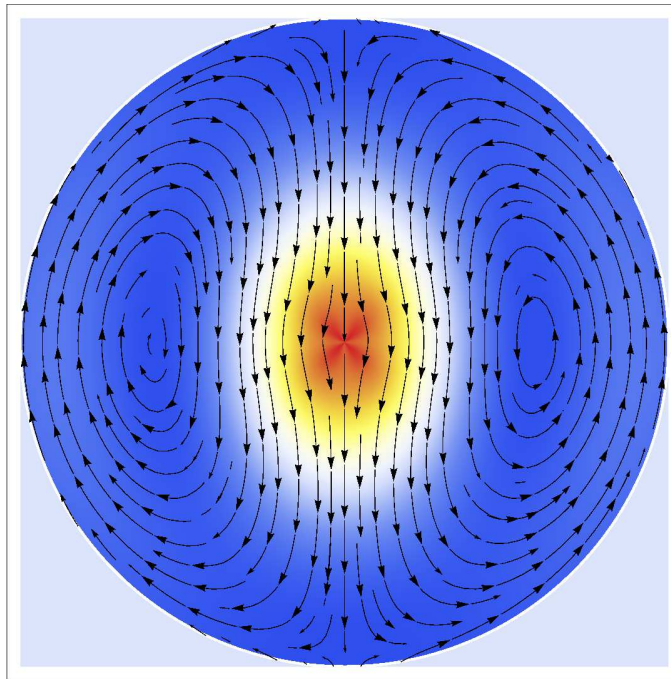


FIG. 5: Real part of the electric field lines (arrows) from Mie theory (*i.e.* from eqs.(11) or (12)) plotted on a background (colour- red maximum) of the internal electric field intensity plot excited by a  $n = 1$ ,  $m = 0$  electric incident field at the anapole point of  $D = 204\text{nm}$  for a wavelength of  $\lambda_b = 550\text{nm}$ .

## V. CONCLUSIONS

The approach we have described to achieve an understanding of the scattering properties of high index dielectric spheres, and in particular of their anapole excitations, has a number of advantages. Firstly, it relies only on the knowledge of the positions of the relevant complex resonances calculated from Mie theory. Secondly, it incorporates an analytically determined phase term, without which a very large number of terms in the product over resonances would be required to achieve accuracy. Thirdly, it does not require the evaluation of inner products or normalisation factors for different resonant modes, which have proved problematic for other approaches. We have shown that, with a small number of the terms relevant to a given sphere diameter range, it can yield information about scattering behaviour of good accuracy, with the simplicity of the formulae used being beneficial to the physical understanding of the phenomena under investigation. The approach is quite general, and will no doubt find applications in a wide range of situations in addition to those studied here.

## ACKNOWLEDGMENTS

Research conducted within the context of the International Associated Laboratory for Photonics between France and Australia. This work has been carried out thanks to the support of the A\*MIDEX project (no. ANR-11-IDEX-0001-02) funded by the Investissements d’Avenir French Government program, managed by the French National Research Agency (ANR). The authors would like to thank Remi Colom, Emmanuel Lassalle, and Nicolas Bonod for helpful discussions.

## VI. APPENDIX: MIE THEORY

The excitation,  $\mathbf{E}_e$ , and scattered,  $\mathbf{E}_s$ , fields can respectively be developed as a multipolar decomposition,

$$\begin{aligned}\mathbf{E}_e(k\mathbf{r}) &= E \sum_{n,m} \left[ e_{nm}^{(e)} \mathbf{N}_{nm}^{(1)}(k\mathbf{r}) + e_{nm}^{(h)} \mathbf{M}_{nm}^{(1)}(k\mathbf{r}) \right] \\ \mathbf{E}_s(k\mathbf{r}) &= E \sum_{n,m} \left[ f_{nm}^{(e)} \mathbf{N}_{nm}^{(+)}(k\mathbf{r}) + f_{nm}^{(h)} \mathbf{M}_{nm}^{(+)}(k\mathbf{r}) \right],\end{aligned}\quad (13)$$

where  $n$  is the electromagnetic angular quantum number, and  $m$  the projection quantum number. The real parameter,  $E$ , determines the strength of the incident field, while multipole wave functions,  $\mathbf{N}_{n,m}(k\mathbf{r})$  and  $\mathbf{M}_{n,m}(k\mathbf{r})$ , are respectively of the ‘electric’ and ‘magnetic’ types (often called TM and TE type fields)<sup>12</sup>, and their coefficients are respectively distinguished with  $(e)$  and  $(h)$  superscripts. The superscript,  $(1)$  on the multipolar fields in eq.(13) denotes regular type fields described by spherical Bessel functions, whereas  $(+)$ ,  $(-)$  refers to fields with outgoing (incoming) boundary conditions (Hankel type fields).

The  $T_n$  functions of Mie theory are meromorphic functions of frequency and constitutive parameters that relate the scattered field coefficients,  $f_{nm}$ , to excitation field coefficients,  $e_{nm}$ ,

$$f_{nm} = T_n e_{nm}. \quad (14)$$

Although incident and scattered fields are very useful from a response function standpoint, it is also to work with the *total fields* that are actually present in the particle plus field system. The partial wave representations of the total field inside the particle,  $\mathbf{E}_{\text{int}}$ , and the total external, field,  $\mathbf{E}_t$ , are respectively,

$$\mathbf{E}_{\text{int}} = E \sum_{n,m} \left[ s_{nm}^{(e)} \mathbf{N}_{nm}^{(1)}(k_s \mathbf{r}) + s_{nm}^{(h)} \mathbf{M}_{nm}^{(1)}(k_s \mathbf{r}) \right] \quad (15a)$$

$$\begin{aligned}\mathbf{E}_t &= E \sum_{n,m} \left[ a_{+,nm}^{(e)} \mathbf{N}_{nm}^{(+)}(k\mathbf{r}) + a_{+,nm}^{(h)} \mathbf{M}_{nm}^{(+)}(k\mathbf{r}) \right. \\ &\quad \left. + a_{-,nm}^{(e)} \mathbf{N}_{nm}^{(-)}(k\mathbf{r}) + a_{-,nm}^{(h)} \mathbf{M}_{nm}^{(-)}(k\mathbf{r}) \right].\end{aligned}\quad (15b)$$

The linear relationship between the internal field coefficients and the incident field coefficients is denoted by the matrix,  $\Omega$ , which is diagonal for spherically symmetric problems, For spheres, the internal field response functions,  $\Omega_n$ , relate the internal field coefficients,  $s_{n,m}$ , to the excitation field coefficients,  $e_{n,m}$ ,

$$s_{n,m} = \Omega_n e_{n,m}, \quad (16)$$

while the  $S$ -matrix relates incoming to outgoing components of the total external field,

$$a_{+,n,m} = S_n a_{-,n,m}. \quad (17)$$

The  $T$ ,  $S$ , and  $\Omega$  functions have exact expressions in Mie theory,

$$\Omega_n = \frac{1}{D_n}, \quad S_n = -\frac{N_{S,n}}{D_n}, \quad T_n = -\frac{N_{T,n}}{D_n}, \quad (18)$$

where the numerator functions can be expressed,

$$N_{S,n}^{(e)} \equiv z \frac{\varepsilon_s j_n(\rho_s z) \xi'_{-,n}(z) - \psi'_n(\rho_s z) h_{-,n}(z)}{i\rho_s} \quad (19a)$$

$$N_{S,n}^{(h)} \equiv z \frac{\mu_s j_n(\rho_s z) \xi'_{-,n}(z) - \psi'_n(\rho_s z) h_{-,n}(z)}{i\mu_s}, \quad (19b)$$

$$N_{T,n}^{(e)} \equiv z \frac{\varepsilon_s j_n(\rho_s z) \psi'_n(z) - \psi'_n(\rho_s z) j_n(z)}{i\rho_s} \quad (19c)$$

$$N_{T,n}^{(h)} \equiv z \frac{\mu_s j_n(\rho_s z) \psi'_n(z) - \psi'_n(\rho_s z) j_n(z)}{i\mu_s}, \quad (19d)$$



and ‘denominator’ functions expressed,

$$D_n^{(e)} \equiv z \frac{\varepsilon_s j_n(\rho_s z) \xi'_{+,n}(z) - \psi'_n(\rho_s z) h_{+,n}(z)}{i\rho_s} \quad (20a)$$

$$D_n^{(h)} \equiv z \frac{\mu_s j_n(\rho_s z) \xi'_{+,n}(z) - \psi'_n(\rho_s z) h_{+,n}(z)}{i\mu_s} . \quad (20b)$$

In Mie theory, the internal field coefficient factors are traditionally defined,  $\Omega_n^{(e)} \equiv d_n$  and  $\Omega_n^{(h)} \equiv c_n$ .

The  $\psi_n$  and  $\xi_{n,\pm}$  are Riccati spherical Bessel functions,  $\psi_n(z) \equiv z j_n(z)$ , and  $\xi_{n,\pm}(z) \equiv z h_n^{(\pm)}(z)$ . Here, the  $\varepsilon_s$  and  $\mu_s$  are the relative constitutive parameters with respect to the background media,

$$\mu_s \equiv \frac{\mu_{r,s}}{\mu_{r,b}} \quad \varepsilon_s \equiv \frac{\varepsilon_{r,s}}{\varepsilon_{r,b}} , \quad (21)$$

and  $\rho_s$  is the refractive contrast with respect to the background medium,

$$\rho_s \equiv \sqrt{\varepsilon_s \mu_s} = \sqrt{\frac{\varepsilon_{r,s} \mu_{r,s}}{\varepsilon_{r,b} \mu_{r,b}}} . \quad (22)$$

Given the Cauchy residue theorem, a comparison of eqs.(8) and (18), leads to the following residues of the internal field coefficients,  $r_{n,\alpha}^{(\Omega,e,h)}$ ,

$$r_{n,\alpha}^{(\Omega)} = \frac{2e^{2iz_{n,\alpha}}}{\left. \frac{d}{dz} D_n(z) \right|_{z=z_{n,\alpha}}} , \quad (23)$$

which following analytic manipulations results in,

$$\begin{aligned} \frac{2i\rho_s e^{2iz_{n,\alpha}}}{r_{n,\alpha}^{(\Omega,e)}} &= z_\alpha^2 h_{+,n}(z_\alpha) j_n(\rho_s z_\alpha) \varepsilon_s (\mu_s - 1) \\ &\quad + (\varepsilon_s - 1) \left[ \xi'_{+,n}(z_\alpha) \psi'_n(\rho_s z_\alpha) \right. \\ &\quad \quad \left. + n(n+1) h_{+,n}(z_\alpha) j_n(\rho_s z_\alpha) \right] \\ \frac{2i\mu_s e^{2iz_{n,\alpha}}}{r_{n,\alpha}^{(\Omega,h)}} &= z_\alpha^2 h_{+,n}(z_\alpha) j_n(\rho_s z_\alpha) \mu_s (\varepsilon_s - 1) \\ &\quad + (\mu_s - 1) \left[ \xi'_{+,n}(z_\alpha) \psi'_n(\rho_s z_\alpha) \right. \\ &\quad \quad \left. + h_{+,n}(z_\alpha) j_n(\rho_s z_\alpha) n(n+1) \right] , \end{aligned} \quad (24)$$

for electric and magnetic multipole resonant states respectively. Analogous comparisons give for the residues,  $r_{n,\alpha}$ , of the  $T$ -matrix in eq.(6),

$$r_{n,\alpha} = -\frac{2N_{T,n}(z_{n,\alpha}) i e^{2iz_{n,\alpha}}}{\left. \frac{d}{dz} D_n(z) \right|_{z=z_{n,\alpha}}} \equiv \frac{2i e^{2iz_{n,\alpha}}}{\mathcal{N}_{n,\alpha}^2} , \quad (25)$$

where  $\mathcal{N}_{n,\alpha}$  correspond to the resonant state ‘normalisation’ factors and for the electric and magnetic modes are respectively given by,

$$\begin{aligned} \left[ \mathcal{N}_{n,\alpha}^{(e)} \right]^2 &= \xi_{+,n}^2 \left( z_{n,\alpha}^{(e)} \right) (\mu_s - 1) \\ &\quad + \left\{ \left[ \xi'_{+,n} \left( z_{n,\alpha}^{(e)} \right) \right]^2 + \frac{n(n+1)}{\varepsilon_s} h_{+,n}^2 \left( z_{n,\alpha}^{(e)} \right) \right\} (\varepsilon_s - 1) \\ \left[ \mathcal{N}_{n,\alpha}^{(h)} \right]^2 &= \xi_{+,n}^2 \left( z_{n,\alpha}^{(h)} \right) (\varepsilon_s - 1) \\ &\quad + \left\{ \left[ \xi'_{+,n} \left( z_{n,\alpha}^{(h)} \right) \right]^2 + \frac{n(n+1)}{\mu_s} h_{+,n}^2 \left( z_{n,\alpha}^{(h)} \right) \right\} (\mu_s - 1) . \end{aligned} \quad (26)$$

which given the differences in notation and conventions simplify to the normalization expressions derived in ref.<sup>13</sup> when restricted to the special case of null permeability contrast, *i.e.*  $\mu_s = 1$ .

It is important to keep in mind that resonant states have important and somewhat unfamiliar properties when compared with the much more common Hermitian spectral analysis of closed conserving systems. Notably, residue/normalisation factors like  $\mathcal{N}_{n,\alpha}$ , are complex numbers so that  $\mathcal{N}_{n,\alpha}^2 \neq |\mathcal{N}_{n,\alpha}|^2$ .

The expressions  $I_n$  and  $J_n$  for determining the average internal field in eq.(3) are found by analytically evaluating the following integrals for the internal fields:

$$\begin{aligned} \frac{2\rho_s^2}{z} I_n &\equiv \frac{2\rho_s^2}{z} \int_0^z \{j_n^2(\rho_s \eta) n(n+1) + \psi_n'^2(\rho_s \eta)\} d\eta \\ &= \psi_n'(\rho_s z) [\psi_n'(\rho_s z) + j_n(\rho_s z)] \\ &\quad + (\rho_s^2 z^2 - n(n+1)) j_n^2(\rho_s z) \end{aligned} \quad (27a)$$

$$\begin{aligned} \frac{2\rho_s^2}{z} J_n &\equiv \frac{2\rho_s^2}{z} \int_0^z j_n^2(\rho_s \eta) \eta^2 d\eta \\ &= \psi_n'(\rho_s z) [\psi_n'(\rho_s z) - j_n(\rho_s z)] \\ &\quad + (\rho_s^2 z^2 - n(n+1)) j_n^2(\rho_s z) . \end{aligned} \quad (27b)$$

\* email : brian.stout@fresnel.fr

<sup>1</sup> Dubovik, V.M. *et al.*, *Phys. Rep.*, 187 (1990) 145.

<sup>2</sup> Leung, P.T. *et al.*, *Phys. Rev. A*, 49(1994) 3057.

<sup>3</sup> Miroschnichenko A.E. *et al.*, *Nature Comm.*, 6 (2015) 8069.

<sup>4</sup> Wei, L. *et al.*, *Optica*, 3 (2016) 799.

<sup>5</sup> Kivshar, Y. *et al.*, *Opt. & Ph. News*, (January 2017) 24.

<sup>6</sup> Powell, D. *Phys. Rev. Applied*, 7 (2017) 034006.

<sup>7</sup> Whittaker, E.T. & Watson, G.N., *A Course of Modern Analysis*, Cambridge U.P. , Cambridge (1965) p. 136.

<sup>8</sup> King, F.W., *Hilbert Transforms, Vol. 2*, Cambridge U.P. , Cambridge (2009) pp. 102-105.

<sup>9</sup> Garcia-Calderon, G *et al.*, *Nuclear Phys.*, A265 (1976) 443.

<sup>10</sup> Grigoriev, V., *Phys. Rev. A*, 88 (2013) 011803(R).

<sup>11</sup> Stout, B. *et al.*, *JOSA A*, 25, (2008) p.2549.

<sup>12</sup> Moine, O. and Stout B., *JOSA B*, 22, (2005) p.1620.

<sup>13</sup> Muljarov, E and Langbein, A.W., *Phys. Rev. B*, 94 (2016) 235438.